Increase Power Grid Stability Using Dual-Excited Synchronous Generator

Alireza Akram[1] and Hamid Yaghobi[1•]

***Abstract*— Transient stability in interconnected power systems remains a pivotal concern for operators, particularly amidst the ever-expanding and intricate nature of modern power grids. This study delves into a novel approach to bolstering power grid stability by proposing the implementation of dual-excited synchronous generators (DESGs). Unlike conventional synchronous generators, DESGs feature dual windings on the rotor, strategically positioned to optimize performance and stability. This paper presents a thorough assessment of synchronous generators and DESGs under varying fault conditions, including three-phase to ground, two-phase to ground, and more. Leveraging advanced simulation techniques in Matlab/Simulink, the dynamic behavior and stability of these generators are meticulously analyzed. The results unveil a paradigm shift: DESGs exhibit superior stability and dynamic performance compared to their conventional counterparts across diverse fault scenarios. By harnessing the advantages of DESGs, including enhanced efficiency, the overall stability and reliability of power grids can be significantly augmented. In summary, this study not only sheds light on the critical importance of power grid stability but also presents a promising solution in the form of DESGs. By pushing the boundaries of traditional generator technology, this research paves the way for a more resilient and efficient electrical infrastructure.**

***Index Terms*—Synchronous generator, dual excited synchronous generator, rotor angle, stability.**

NOMENCLATURE

T_{damp}	friction-induced torque of the generator
T_{mech}	Mechanical torque of the generator
P	Number of poles
V_q , V_d	Voltage on the q-axis and d-axis of the synchronous generator, respectively.
V_0	Voltage on the zero (0) axis of the synchronous generator.
$parent\theta_r(t)$	The angle between the r-axis of the rotor and the aa-axis of the stator, in radians.
$\omega_r(t)$	Rotor angular velocity.
ψ_q, ψ_d	Flux linkage on the q-axis and d-axis of the synchronous generator, respectively.
ψ_0	Flux linkage on the zero (0) axis of the synchronous generator.
ψ'_{kq} , ψ'_{kd}	Flux linkage for damper windings k on the q-axis and d-axes, respectively.
ψ'_{fq} , ψ'_{fd}	Flux linkage for excitation windings f on the q-axis and d-axis, respectively.
ψ_{mq}	Flux linkage on the q-axis of the synchronous generator for the q-axis.
ψ_{md}	Flux linkage on the d-axis of the synchronous generator for the d-axis.
i_q , i_d	Current on the q-axis and d-axis of the synchronous generator, respectively.
i'_{kq} , i'_{kd}	Curent for damper windings k on the q-axis and d-axis, respectively.
i'_{fq} , i'_{fd}	Current for excitation windings f on the q-axis and d-axis, respectively.
i_0	Current on the zero (0) axis of the synchronous generator.
i_a, i_b, i_c	Phase currents of the synchronous generator (Phase A, Phase B, Phase C).
δ(t)	Rotor angle of the synchronous generator.
P_{em}	Electromagnetic power developed.
T_{em}	Electromechanical torque
r'_{kq}, r'_{kd}	Resistance of damper windings k on the q-axis and d-axis, respectively.
x'_{lkq}, x'_{lkd}	Leakage reactance of damper windings k on the q-axis and d-axis, respectively.
r'_{fq}, r'_{fd}	Resistance of excitation windings f on the q-axis and d-axis, respectively.
x'_{lfq}, x'_{lfd}	Leakage reactance of excitation windings f on the q-axis and d-axis, respectively.
x_{mq}, x_{md}	Mutual reactance on the q-axis and d-axis, respectively.
x_{ls}	Synchronous reactance.
L_{mq}, L_{md}	Self-inductance of the q-axis and d-axis, respectively.
V_a, V_b, V_c	Phase voltages of the synchronous generator (Phase A, Phase B, Phase C).
ψ'_{fq}, ψ'_{fd}	Flux linkages for excitation windings f on the q-axis and d-axis, respectively.
E_{fq}, E_{fd}	Excitation voltages for excitation windings f on the q-axis and d-axis, respectively.
r_s	Stator resistance.
λ_q , λ_d	D-axis and q-axis stability coefficients, respectively.

1 . Faculty of Electrical & Computer Engineering, Semnan University, Semnan, Iran.

• Corresponding author Email: mailto:yaghobi@semnan.ac.ir

I. Introduction

Synchronous generators are foundational components within power grids, serving as vital contributors to both power generation and grid stability. In the face of expanding and increasingly intricate modern power networks, meeting escalating energy demands underscores the paramount importance of ensuring the stability and reliability of synchronous generators [1]- [6]. Efforts aimed at augmenting the efficiency and performance of these generators stand as integral pillars in the progression of sustainable energy technologies. By fostering heightened productivity and bolstering system stability, advancements in these areas carry profound implications for the overall performance of power systems [7]- [10]. Consequently, the imperative arises for the development of methodologies and techniques geared towards fortifying generator stability.

Various conditions can lead to instability in synchronous generators, including phase-to-phase faults, single-phase-to-ground faults, two-phase-to-ground faults, three-phase-to-ground faults, or phase-to-phase faults. Given the significant financial implications of generator incidents and system instability, there is strong motivation to find a solution to enhance the stability of the power grid [11], [12].

Transient stability studies are essential to ensure a power grid can withstand transient conditions following severe disturbances. These studies help determine critical parameters such as relay system characteristics, fault resolution timing, system voltage level, and power transfer capability [13], [14]. Rotor angle instability, induced by load changes, disconnections, and short circuits, is a prominent instability in power grids, underscoring the need for strategies to address it [15].

Efforts to enhance the stability of synchronous generators directly contribute to the overall stability of power systems [12], [16]. Therefore, if an alternative structure of a synchronous generator could be utilized instead of the conventional synchronous generator (CSG), offering greater stability against various faults, the stability of the power system would also increase**.** This alternative structure may be a Dual Excited Synchronous Generator (DESG), which is the focus of this paper**.** Comparative studies between CSGs and DESGs under various fault conditions can play a significant role in examining and evaluating the dynamic performance and stability of the system.

To date, studies have been conducted to investigate the dynamic behavior and stability of Dual Excited Synchronous Generators (DESGs) [17]- [21]. Recent discussions have focused on the control and stability of dual-excited machines Studies have demonstrated that the stability of DESGs can be enhanced by adjusting the angle of DESGs [14]. Dynamic analyses of DESGs under various conditions with different regulators have been conducted using criteria such as the Routh criterion [22], [23]. Notably, the loss of torque or reactive winding fields does not significantly affect system stability. By maintaining similar losses in both field windings, heterogeneous rotor heating can be mitigated, as each rotor winding is controlled independently. Additionally, the angle between field windings has been studied, revealing no significant impact on stability [24]- [35].

This paper simulates conventional synchronous generators and dual-excited synchronous generators using their mathematical equations in MATLAB, applying various types of faults such as single-phase to ground faults, two-phase to ground faults, three-phase to ground faults, and phase-to-phase faults at different time intervals to the terminals of both generators. The stability of these two generators is examined and compared under various fault conditions, with the results indicating that DESGs exhibit better stability compared to CSGs under different applied faults. Considering the direct impact of synchronous generator stability on power system stability, it can be concluded that employing dual-excited synchronous generators instead of traditional synchronous generators can enhance the overall stability of the power system.

II. System Model

The DESG construction, its dynamic model, and the equations used in the simulation of this generator are discussed in this section.

A. Dual-Excited Synchronous Generator Construction

The DESG has two windings in different directions. The two windings are excited independently, and the direction and magnitude of the resulting magnetic field can be controlled arbitrarily. The schematic view of the DESG is illustrated in Fig. 1, where the angle between the windings is less than 90°, the windings have an equal number of turns, and none of the windings are on the d and q axes.

DESG's terminal voltage is generated by applying two alternating voltages with different phases to each winding. This creates a magnetic field in the generator air gap that is the sum of the rotating magnetic field frequency and the rotational frequency of the rotor.

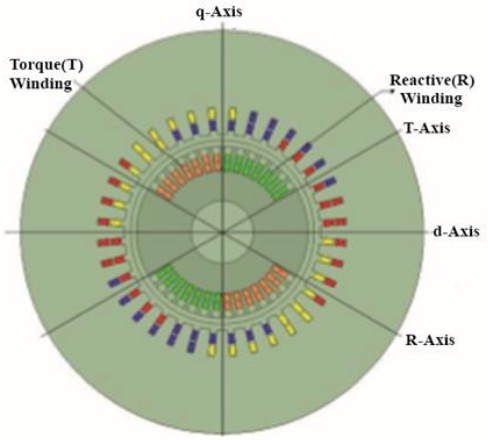

Fig. 1. Schematic view of the dual-excited synchronous generator [2]

B. Dual-Excited Synchronous Generator Dynamic Model and Equations

DESGs have two excitation windings, f1 and f2, which are moved with desired angles θ1 and θ2 from the mechanical axis (axis d). Dual-excited generators can be replaced with two-axis generators (d-q generators) if the interaction between the two excitation windings is negligible. Both machines produce a

magnetic field of the same magnitude and direction [30]. Fig. 2 illustrates the DESG equivalent to the d-q machine.

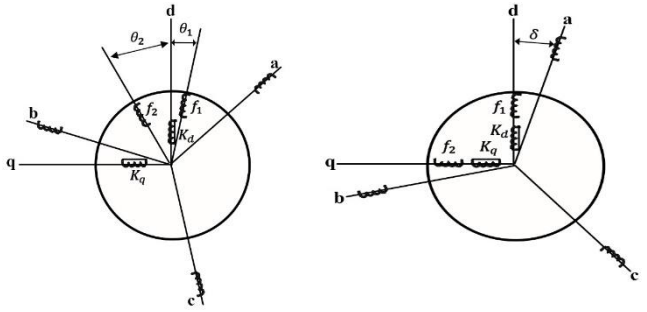

(a) (b)

Fig. 2. The dynamic model of dual-excited synchronous generator. (a) dual-excited machine. (b) d-q machine [36].

The following is a description of the equations of DESG [37]. The equations about DESG are written for the d-q generator. These equations are used to simulate this generator.

$$\begin{aligned} V_q &= \frac{2}{3}\left\{V_a\, cos\theta_r(t) + V_b \cos\left(\theta_r(t) - \frac{2\pi}{3}\right)\right. \\ &\quad \left. +\ V_c \cos\left(\theta_r(t) - \frac{4\pi}{3}\right)\right\} \\ V_d &= \frac{2}{3}\left\{V_a\, sin\theta_r(t) + V_b \sin\left(\theta_r(t) - \frac{2\pi}{3}\right)\right. \\ &\quad \left. + V_c \sin\left(\theta_r(t) - \frac{4\pi}{3}\right)\right\} \\ V_0 &= \frac{1}{3}(V_a + V_b + V_c) \end{aligned} \quad (1)$$

where

$$\theta_r(t) = \int_0^t \omega_r(t)dt + \theta_r(0) \quad elec \cdot rad \quad (2)$$

In equation (1), $\theta_r(t)$ is the angle between the r-axis of the rotor and the a-axis of the stator, and ω_r(t) is the velocity of the rotor angle. There are two excitation windings and two damping windings on the d and q axes of the DESG. Here are the integral equations for the flux linkages of the windings [37].

$$\psi_q = \omega_b \int \left\{v_q - \frac{\omega_r}{\omega_b}\psi_d + \frac{r_s}{x_{ls}}(\psi_{mq} - \psi_q)\right\} dt \quad (3)$$

$$\psi_d = \omega_b \int \left\{v_d + \frac{\omega_r}{\omega_b}\psi_q + \frac{r_s}{x_{ls}}(\psi_{md} - \psi_d)\right\} dt \quad (4)$$

$$\psi_0 = \omega_b \int \left\{v_0 - \frac{r_s}{x_{ls}}\psi_0\right\} dt \quad (5)$$

Equations (6) and (7) can also be used to calculate flux linkages for damping windings [37].

$$\psi'_{kq} = \frac{\omega_b r'_{kq}}{x'_{lkq}} \int (\psi_{mq} - \psi'_{kq})\, dt \quad (6)$$

$$\psi'_{kd} = \frac{\omega_b r'_{kd}}{x'_{lkd}} \int (\psi_{md} - \psi'_{kd})\, dt \quad (7)$$

The following equations are used to calculate the flux linkages of the generator excitation windings [37].

$$\psi'_{fq} = \frac{\omega_b r'_{fq}}{x_{mq}} \int \left\{E_{fq} + \frac{x_{mq}}{x'_{lfq}}(\psi_{mq} - \psi'_{fq})\right\} dt \quad (8)$$

$$\psi'_{fd} = \frac{\omega_b r'_{fd}}{x_{md}} \int \left\{E_{fd} + \frac{x_{md}}{x'_{lfd}}(\psi_{md} - \psi'_{fd})\right\} dt \quad (9)$$

The variables used in the expressed equations are defined as follows: The following is a description of the flux linkages of the windings on the d and q axes [37].

$$\psi_{mq} = \omega_b L_{mq}(i_q + i'_{kq} + i'_{fq}) \quad (10)$$

$$\psi_{md} = \omega_b L_{md}(i_d + i'_{kd} + i'_{fd}) \quad (11)$$

Also, excitation voltages in the two axes d and q can be defined as follows [37]:

$$E_{fq} = x_{mq}\frac{V'_{fq}}{r'_{fq}} \quad (12)$$

$$\psi_{md} = \omega_b L_{md}(i_d + i'_{kd} + i'_{fd}) \quad (13)$$

A stator winding flux linkage is also defined by Equations (14)-(16).

$$\psi_q = x_{ls} i_q + \psi_{mq} \quad (14)$$

$$\psi_d = x_{ls} i_d + \psi_{md} \quad (15)$$

$$\psi_0 = x_{ls} i_0 \quad (16)$$

Excitation winding flux linkages can also be defined as follows [37]:

$$\psi'_{fq} = x'_{lfq} i'_{fq} + \psi_{mq} \quad (17)$$

$$\psi'_{fd} = x'_{lfd} i'_{fd} + \psi_{md} \quad (18)$$

Damping winding flux linkages are expressed in Equations (19) and (20) as follows:

$$\psi'_{fq} = x'_{lfq} i'_{fq} + \psi_{mq} \quad (19)$$

$$\psi'_{fd} = x'_{lfd} i'_{fd} + \psi_{md} \quad (20)$$

In terms of the total winding flux linkages, the flux linkages of the windings on the d and q axes are as follows [37] :

$$\psi_{mq} = x_{MQ}\left(\frac{\psi_q}{x_{ls}} + \frac{\psi'_{kq}}{x'_{lkq}} + \frac{\psi'_{fq}}{x'_{lfq}}\right) \quad (21)$$

$$\psi_{md} = x_{MD}\left(\frac{\psi_d}{x_{ls}} + \frac{\psi'_{kd}}{x'_{lkd}} + \frac{\psi'_{fd}}{x'_{lfd}}\right) \quad (22)$$

$$\frac{1}{x_{MQ}} = \frac{1}{x_{mq}} + \frac{1}{x'_{lkq}} + \frac{1}{x'_{lfq}} + \frac{1}{x_{ls}} \quad (23)$$

$$\frac{1}{x_{MD}} = \frac{1}{x_{md}} + \frac{1}{x'_{lkd}} + \frac{1}{x'_{lfd}} + \frac{1}{x_{ls}} \quad (24)$$

The following are the equations for the generator winding currents [37].

$$i_q = \frac{\psi_q - \psi_{mq}}{x_{ls}} \quad (25)$$

$$i_d = \frac{\psi_d - \psi_{md}}{x_{ls}} \quad (26)$$

In addition, through the following equations, the winding currents of the damper located on the rotor in the d-q axis can be calculated [37].

$$i'_{kq} = \frac{\psi'_{kq} - \psi_{mq}}{x'_{lkq}} \quad (27)$$

$$i'_{kd} = \frac{\psi'_{kd} - \psi_{md}}{x'_{lkd}} \quad (28)$$

Generator excitation currents can also be calculated as follows [37]:

$$i'_{fq} = \frac{\psi'_{fq} - \psi_{mq}}{x'_{lfq}} \quad (29)$$

$$i'_{fd} = \frac{\psi'_{fd} - \psi_{md}}{x'_{lfd}} \quad (30)$$

The following transformations can be performed for stator winding currents [37].

$$i^s{}_q = i_q \cos\theta_r(t) + i_d \sin\theta_r(t) \quad (31)$$

$$i^s{}_d = -i_q \sin\theta_r(t) + i_d \cos\theta_r(t) \quad (32)$$

$$i_a = i^s{}_q + i_0 \quad (33)$$

$$i_b = -\frac{1}{2} i^s{}_q - \frac{1}{\sqrt{3}} i^s{}_d + \quad (34)$$

$$i_c = -\frac{1}{2} i^s{}_q - \frac{1}{\sqrt{3}} i^s{}_d + i_0 \quad (35)$$

In the case of a p-pole machine, the expanded electromagnetic power can be calculated without accounting for ohmic losses and the rate of change of magnetic energy [37]:

$$P_{em} = \frac{3}{2}\frac{p}{2}\omega_{rm}(\lambda_d i_q - \lambda_q i_d) \quad W \quad (36)$$

By dividing (36) by the mechanical speed of the rotor, the electromechanical torque can be calculated as follows [37]:

$$T_{em} = \frac{P_{em}}{\omega_{em}} = \frac{3}{2}\frac{P}{2}(\lambda_d i_q - \lambda_q i_d) = \frac{3}{2}\frac{P}{2\omega_b}(\psi_d i_q - \psi_q i_d) \quad N \cdot m \quad (37)$$

T_{em} has a positive value for engine performance of the machine and a negative value for its generator performance. The motor contract defines net acceleration torque as $T_{em} + T_{mech} - T_{damp}$ along the rotor rotation. T_{em} is positive in the motor mode, and negative in the generator mode. If the machine is rotated in the generator mode by an initial actuator, T_{mech} will be negative, while T_{damp}, the friction-induced torque, will act in the opposite direction of the rotor rotation. This pure accelerator torque will have the following relationship with the inertial torque [37]:

$$T_{em} + T_{mech} - T_{damp} = J\frac{d\omega_{rm}(t)}{dt} = \frac{2J}{P}\frac{d\omega_{rm}(t)}{dt} \quad N \cdot m \quad (38)$$

In addition, the rotor angle and reactive and active power of the generator are calculated as follows [37]:

$$\delta(t) = \theta_r(t) - \theta_e(t) = \int_0^t [\omega_r(t) - \omega_e(t)]\,dt + \theta_r(0) - \theta_e(0) \quad (39)$$

$$\psi_d = \omega_b \int \left\{ v_d + \frac{\omega_r}{\omega_b}\psi_q + \frac{r_s}{x_{ls}}(\psi_{md} - \psi_d) \right\} dt \quad (40)$$

$$\psi_0 = \omega_b \int \left\{ v_0 - \frac{r_s}{x_{ls}}\psi_0 \right\} dt \quad (41)$$

III. SYMULATION

This section investigates and contrasts the stability of Conventional Synchronous Generators (CSGs) and Dual-Excited Synchronous Generators (DESGs) under diverse fault scenarios, encompassing three-phase to ground, two-phase to ground, single-phase to ground, and phase-to-phase faults. Fig. 3 provides a comprehensive overview of the dual-excited synchronous generator model within the Matlab/Simulink software. This section focuses on simulating the d-q generator model. The windings of the generators in this simulation are connected in a star (wye) configuration.

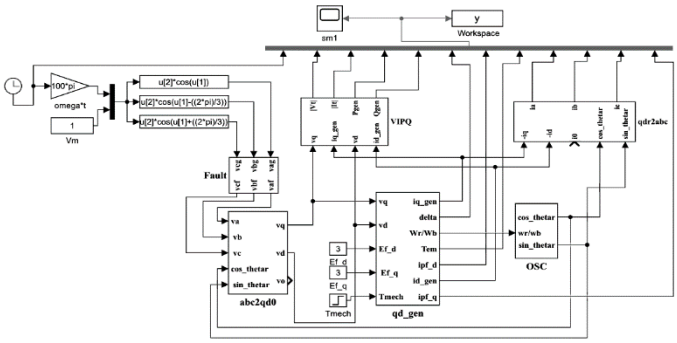

Fig. 3. Full view of the dual-excited synchronous machine model in the Simulink

A. Simulation Condition

During the simulation of the CSG and DESG in this paper, the standard parameters of both generators were the same, and the fundamental electrical parameters of the generators were determined based on these values. In addition to the different number of excitation windings, the two generators have different weights. However, it appears that the weight does not have a considerable impact on stability. This issue can be addressed in future research. Table1 shows the identical parameters of the two simulated synchronous generators.

TABLE I

Identical Parameters of the Two Simulated Synchronous Generators Standard Parameters of Generators

d-axis	q-axis
$x_d = 1.0495\ pu$	$x_q = 0.6313\ pu$
$x'_d = 0 \cdot 3320\ pu$	$x'_q = 0 \cdot 394\ pu$
$x''_d = 0 \cdot 1963\ pu$	$x''_q = 0 \cdot 2496\ pu$
$T'_{do} = 3.7729\ s$	$T'_{qo} = 0.18\ s$
$T''_{do} = 0.0238\ s$	$T''_{qo} = 0.0334\ s$
Parameters of stator	
$r_s = 0 \cdot 00636\ \ pu$	$x_{ls} = 0 \cdot 1235\ \ pu$

The fundamental electrical parameters for the CSG and DESG are given in Table II..

TABLE II

Fundamental Electrical Parameters for the Two Simulated Synchronous Generators

Conventional Synchronous Generator	
d-axis	q-axis
$x_{md} = 0.926\ pu$	$x_{mq} = 0.5078\ pu$
$x'_{lfd} = 0 \cdot 2691\ pu$	$x'_{lkq} = 0 \cdot 1678\ pu$
$x'_{lkd} = 0 \cdot 1119\ pu$	$r'_{kq} = 0 \cdot 053\ pu$
$r'_{kd} = 0 \cdot 03578\ pu$	
$r'_{fd} = 0 \cdot 0084\ pu$	
Dual-excited synchronous generator	
d-axis	q-axis
$x_{md} = 0.926\ pu$	$x_{mq} = 0.5078\ pu$
$x'_{lfd} = 0 \cdot 2691\ pu$	$x'_{lfq} = 0 \cdot 578\ pu$
$x'_{lkd} = 0 \cdot 1119\ pu$	$x'_{lkq} = 0 \cdot 2363\ pu$
$r'_{kd} = 0 \cdot 03578\ pu$	$r'_{kq} = 0 \cdot 0574\ pu$
$r'_{fd} = 0 \cdot 0084\ pu$	$r'_{fq} = 0 \cdot 00076\ pu$

According to Table I, the standard parameters of the generators can be used to calculate the fundamental electrical parameters of the generators [36] - [38].

The nominal values of the generators are given in Table III [38]. Additionally, in both generators, the coefficient of damping related to the friction-induced torque is equal to zero. ($D_\omega = 0$), And the constant inertia value is equal to 7.11 seconds ($H = 7.11\ s$). The generator outputs in this article have been expressed per unit (p.u.) based on their nominal values, as presented in Table III.

TABLE III
Nominal Values of the Simulated Generators

Type of generators	Apparent power (S)	Voltage(V)	Current (I)	Speed(N)	Frequency (F)
CSG	6250 KVA	4160 V	867.41 A	360 RPM	60 Hz
DESG	8800 KVA	4160 V	1.221 KA	360 RPM	60 Hz

In the simulation conducted in this paper, single-phase to ground, two-phase to ground, three-phase to ground, and phase-to-phase faults were applied to both generators for various durations, and their stability was investigated. Subsequently, explanations regarding these faults are provided.

All of these faults were applied to the terminal of the generators in the simulation. The fault resistances were considered to be 0.001 ohms, and the ground resistance was assumed to be 0.01 ohms. The three-phase terminal voltages of both generators can be observed in Fig. 4.

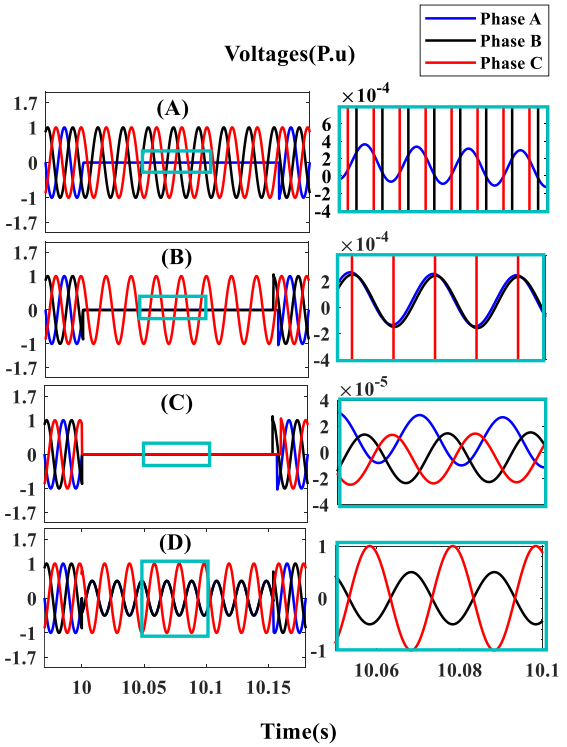

Fig. 4. The three-phase terminal voltages of CSG and DESG under different short-circuit fault conditions. Faults were applied at 10 seconds and cleared at 10.15 seconds. The figures on the right show enlarged views of the time interval of the phases affected by the fault. A) Single-phase-to-ground fault B) Two-phase-to-ground fault C) Three-phase-to-ground fault D) Phase-to-phase fault

As depicted in Fig. 4, different faults were applied to the generator terminals at second 10, and they were cleared at second 10.15. The variations in the three-phase terminal voltages of the generators can be observed during this time interval.

B. Simulation Results

In this section, first, the simulation results of the simulated generators in nominal and stable conditions are examined, and then, by applying different faults to generators' terminals, the simulation results of the generators under different faults are examined.

B. I. Simulation Results of the Generators in Nominal and Stable Conditions

In this section, the simulation outputs of CSGs and DESGs under nominal conditions are examined. Fig. 5 shows the instantaneous stator voltage for CSGs and DESGs under rated conditions. Both generators have an instantaneous stator voltage of 1 pu, as can be seen. Also, Fig. 6 illustrates the instantaneous stator current for CSGs and DESGs under rated conditions. In CSGs, the stator current is equal to 1 pu, and in DESGs, it is equal to 1.491 pu. The reason for the higher stator instantaneous current in DESGs is that they have one more excitation winding; thus, they produce greater flux than CSGs with the same standard parameter values.

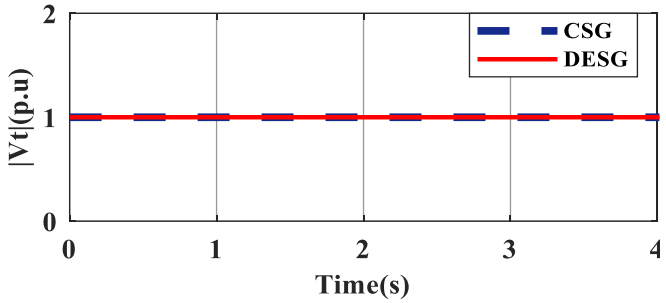

Fig. 5. The instantaneous voltage of conventional and dual-excited synchronous generators under rated conditions.

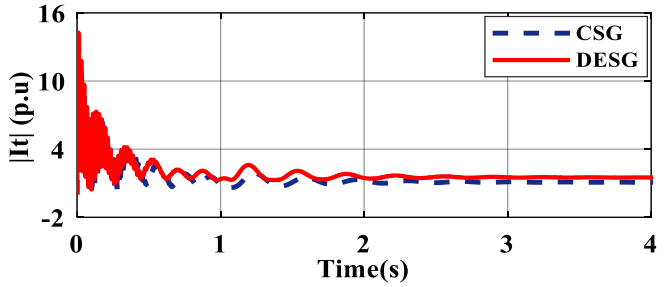

Fig. 6. The instantaneous current of conventional and dual-excited synchronous generators under rated conditions.

Also, as shown in Fig. 7, CSG and DESG have different rotor angles under rated conditions. In Fig. 6, the final rotor angle in the CSG is 64.64 degrees, while it is 57.05 degrees in the DESG. The reason is that the rotor angle swings are different between the two generators (), from when the generator is started up until it reaches the synchronous speed; this explains why the rotor angles of the two generators differ.

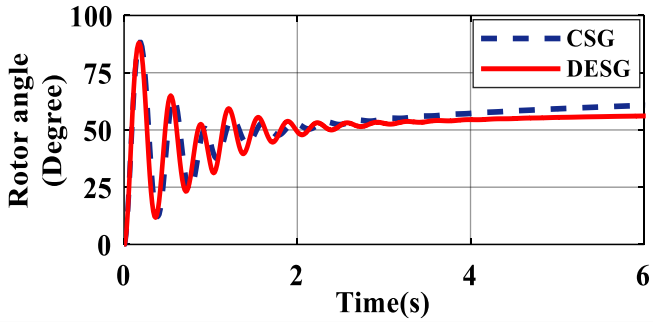

Fig.7. The rotor angle of conventional and dual-excited synchronous generators under rated conditions.

B. II. Simulation Results of the Generators Under Three-Phase to Ground Fault

Fig. 8 shows that by applying a three-phase to ground fault to the terminals of both generators for 0.1 seconds, from 10 to 10.1 seconds, both generators swing slightly and return to stability. Increasing the fault time in Fig. 8 to 0.136 seconds shows that the CSG completely swings and loses its stability, but the DESG reaches its steady-state value after its swings and becomes stable. As soon as the fault time reaches 0.15 seconds, both generators become unstable. Therefore, the CSG was able to withstand the three-phase to ground fault for 0.136 seconds and did not lose its stability, while this time was 0.15 seconds for the DESG. This indicates the greater stability of the DESG compared to the CSG under three-phase to ground fault.

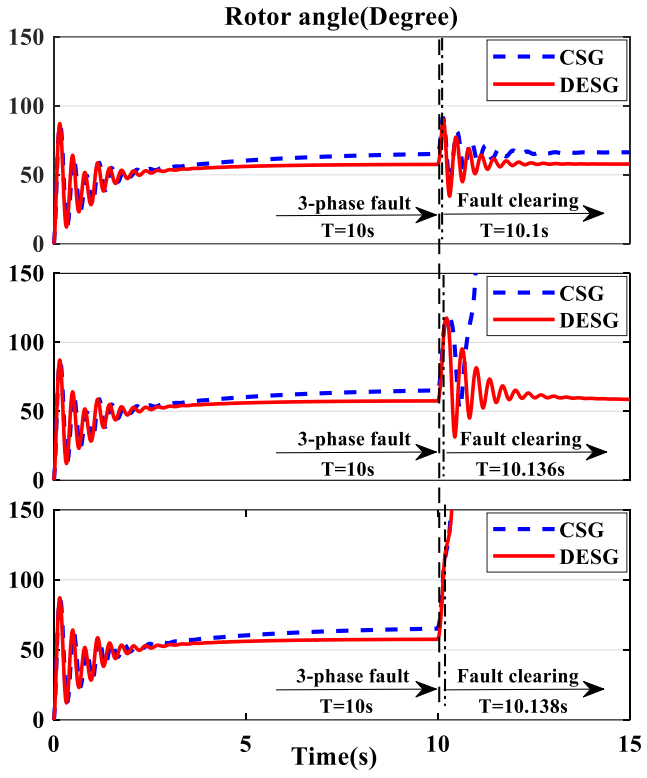

Fig. 8. The rotor angle of conventional and dual-excited synchronous generators under a three-phase to ground fault that occurs in the 10th second with a fault duration ranging from 0.1 to 0.15 seconds.

B. III. Simulation Results of the Generators Under Two-Phase to Ground Fault

Fig. 9 shows that by applying a two-phase to ground fault to the terminals of both generators for 0.1 seconds, from 10 to 10.1 seconds, both generators swing slightly and return to stability. By increasing the fault time in Fig. 9 to 0.14 seconds, it is clear that the CSG completely swings and loses stability, but the DESG reaches its steady-state value after its swings and remains stable. Both generators become unstable as soon as the fault time reaches 0.17 seconds. Thus, the CSG was able to withstand the two-phase to ground fault for 0.14 seconds without losing stability, while the DESG became unstable after 0.17 seconds. Accordingly, the DESG is more stable than the CSG under two-phase to ground fault conditions.

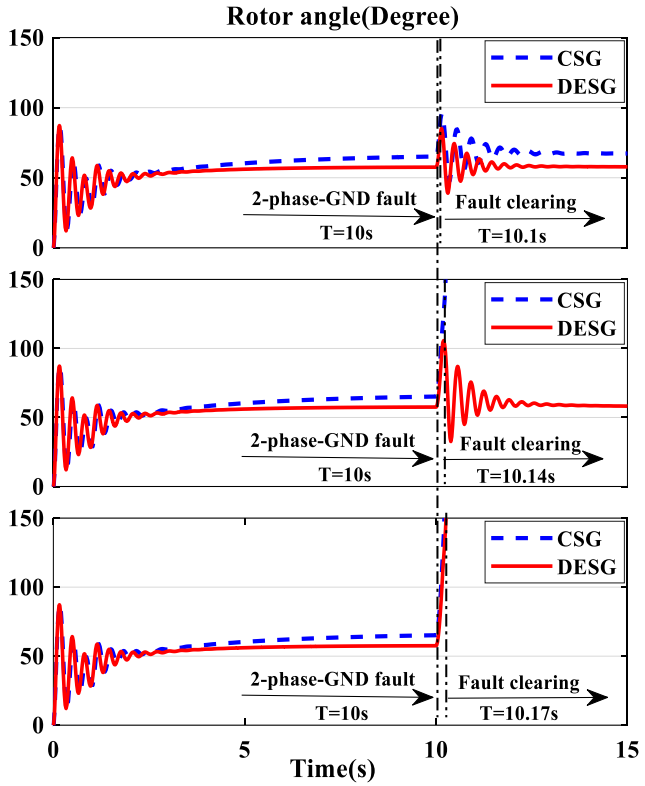

Fig. 9. The rotor angle of conventional and dual-excited synchronous generators under a two-phase to ground fault occurs in the 10th second with a fault duration ranging from 0.1 to 0.17 seconds.

B. IV. Simulation Results of the Generators Under a Single-Phase to Ground Fault

Fig. 10 shows that by applying a single-phase ground fault to the terminals of both generators for 0.1 seconds, from 10 to 10.1 seconds, both generators swing slightly and then return to stability. As the fault time in Fig. 10 increases to 0.22 seconds, it becomes clear that the CSG completely swings and loses stability, while the DESG reaches its steady-state value after its swings and remains stable. As soon as the fault time reaches 0.78 seconds, both generators become unstable. As a result, the CSG was able to tolerate the single-phase to ground fault for 0.22 seconds without losing stability, whereas the DESG became unstable after 0.78 seconds. Therefore, the DESG is more stable than the CSG under single-phase to ground fault conditions.

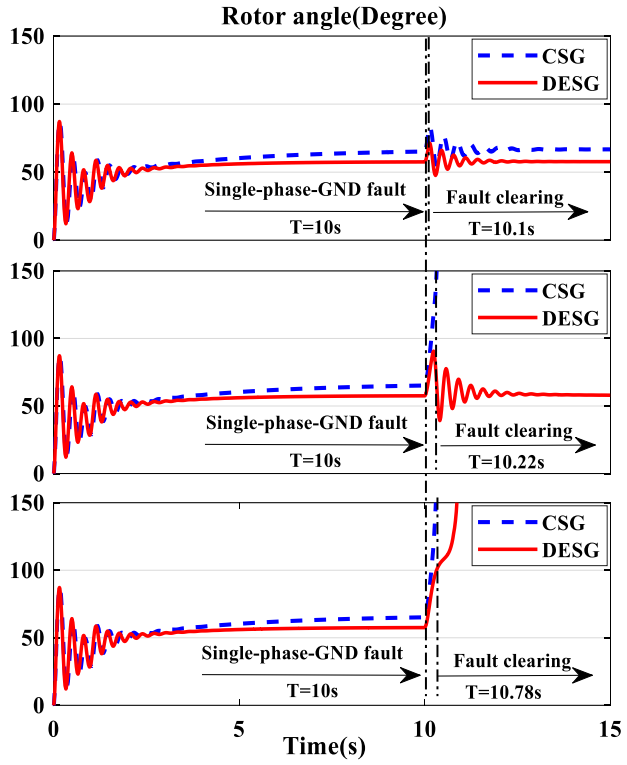

Fig. 10. The rotor angle of conventional and dual-excited synchronous generators under a single-phase to ground fault occurs in the 10th second with a fault duration ranging from 0.1 to 0.78 seconds.

B. V. Simulation Results of the Generators Under a Phase-to-Phase Fault

Fig. 11 illustrates the results of the two generators under phase-to-phase fault conditions.

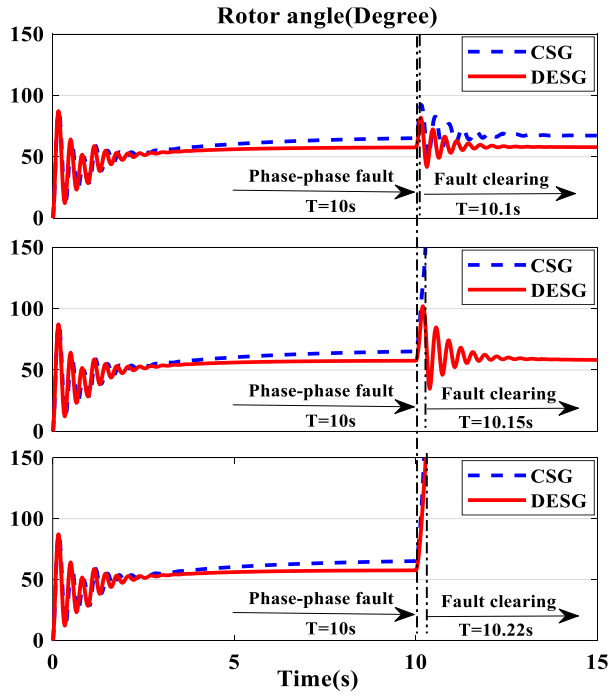

Fig. 11. The rotor angle of conventional and dual-excited synchronous generators under a phase-to-phase fault that occurs in the 10th second with a fault duration ranging from 0.1 to 0.2 seconds.

Phase-to-phase faults are applied to both generators from 10 to 10.1 seconds, causing both generators to swing slightly and then return to stability. The fault time in Fig. 11 increases to 0.15 seconds, and it becomes clear that the CSG completely swings and loses stability, whereas the DESG reaches its steady-state value after its swings and remains stable. Once the fault time reaches 0.2 seconds, both generators become unstable. Therefore, the CSG was able to withstand the phase-to-phase fault for 0.15 seconds without losing stability, whereas the DESG became unstable after 0.2 seconds. Under phase-to-phase fault conditions, the DESG is, therefore, more stable than the CSG.

Furthermore, in this section, a comparison of the active and reactive power of two generators under phase-to-phase fault has also been conducted, the results of which can be observed in Fig. 12 and 13.

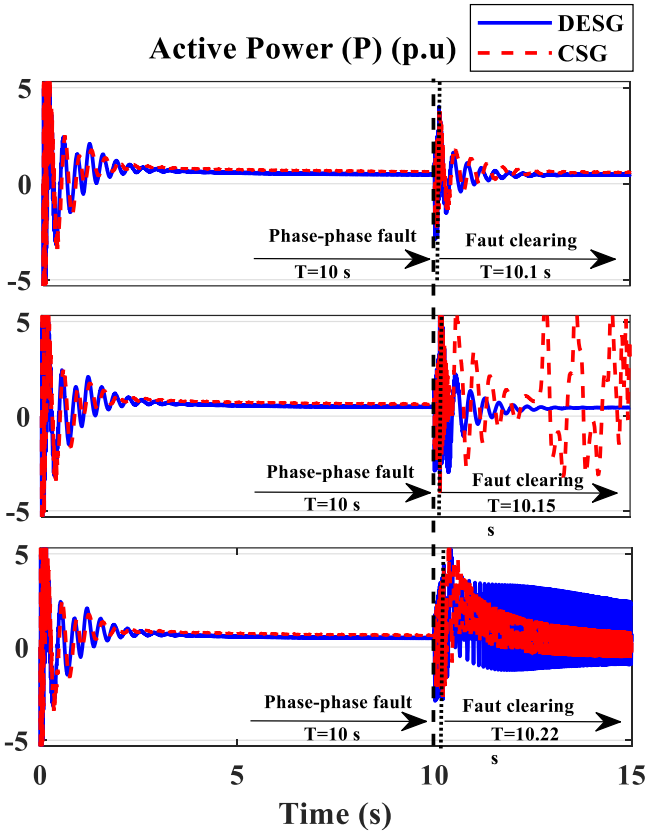

Fig. 12. . The active power of conventional and dual-excited synchronous generators under a phase-to-phase fault that occurs in the 10th second with a fault duration ranging from 0.1 to 0.2 seconds.

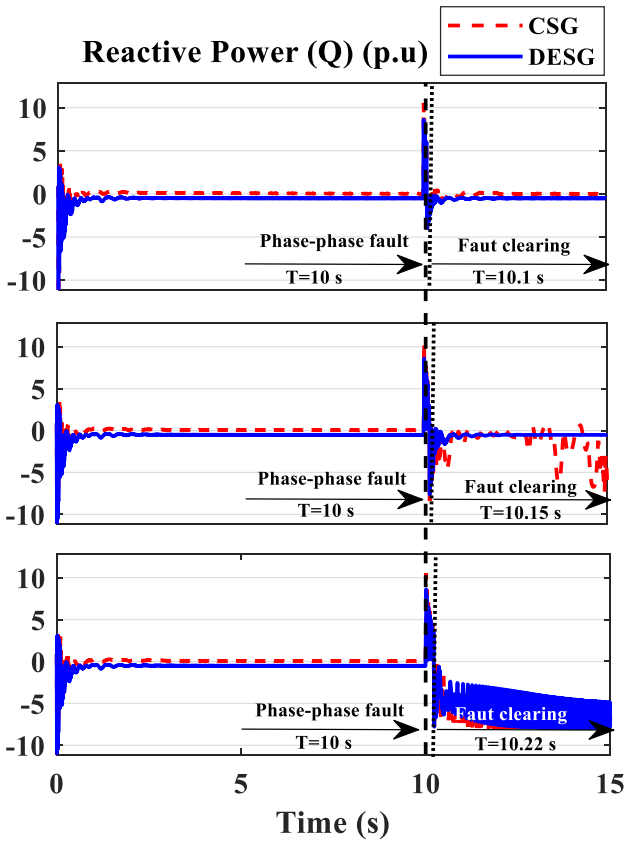

Fig. 13. The reactive power of conventional and dual-excited synchronous generators under a phase-to-phase fault that occurs in the 10th second with a fault duration ranging from 0.1 to 0.2 seconds.

As evident, both generators remain stable in terms of both active and reactive power during the fault application time of 1 second from 10 seconds to 10.1 seconds. With an increase in fault application time to 0.15 seconds, the active and reactive power of the conventional synchronous generator deviate from their stable state and do not return to their nominal value, while the dual-excited synchronous generator remains stable. Upon further increase in fault application time to 0.22 seconds, the powers of both generators deviate from their stable state.

IV. Discussion

Table IV shows how long the CSG and DESG can maintain their stability when facing a variety of faults. According to TableIV, the stability time of the DESG in all four types of faults examined is greater than that of the CSG, indicating that DESGs are more stable than CSGs. Compared to the four types of faults studied, CSG and DESG have the lowest stability under three-phase to ground faults, while, under single-phase to ground faults, they have the highest stability.

Table IV.
Duration of Maintaining the Stability of Two Types of Generators After Clearing the Various Faults

Fault	Generator type	
	CSG	DESG
Single-phase to ground	Up to 220 ms	Up to 780 ms
Two-phase to ground	Up to 140 ms	Up to 170 ms
Phase to phase	Up to 150 ms	Up to 200 ms
Three-phase to ground	Up to 136 ms	Up to 150 ms

V. Conclusion

. As a result of a synchronous generator's instability, other synchronous generators in the power system are also affected. There is a possibility of this situation affecting the power system's stability, even resulting in a shutdown of the power system. Consequently, synchronous generators are important for the stability of the power grid, and increasing their stability increases the grid's stability. The stability of CSG and DESG was assessed in this paper with different fault conditions, including three-phase-to-ground, two-phase-to-ground, single-phase-to-ground, and phase-to-phase faults. According to the results, DESG had better dynamic performance and more stability than CSG. The power grid can therefore be made more reliable and stable under different fault conditions by replacing the CSG with the DESG.

References

[1] A. R. Daniels and Y. B. Lee, "Optimal and suboptimal excitation control of dual-excited synchronous generators", Proc. I. E. E., vol. 123, no. 10, pp. 989-992, 2010.

[2] A. A. Reddy, S. S. Bhat, and R. T. Ugale, "Design and FEM analysis of dual excited synchronous generator." 2017 National Power Electronics Conference (NPEC). IEEE, pp. 302-306, 2017.

[3] R. B. Robinson, "Transient equivalent circuit of the divided winding rotor synchronous machine", Proc. I.E.E., vol. 117, pp. 552-554, 1970.

[4] H. Yaghobi and H. Kafash Haghparas, " Study on application of two different magnetic materials in rotor of cylindrical synchronous generator to produce reluctance torque", Iranian Journal of Electrical & Electronic Engineering, Vol. 11, No.3, pp. 253-264, 2015.

[5] R. Ilka and Y. Alinejad-Beromi, “A Novel Space Reduction Technique for Design Optimization of Permanent Magnet Synchronous Motors”, Modeling and Simulation in Electrical and Electronics Engineering, vol. 2, pp. 1-7, 2022.

[6] A. Ehsani-Seresht, A. Bolourian, and R. RoshanFekr, “Detection of the Misalignment Fault in Non-Electric Rotating Machines Through the Current Signal of a Brushless Direct Current Motor”, Modeling and Simulation in Electrical and Electronics Engineering, vol.2, pp. 11-17, 2022.

[7] R. H. Nelson, T. A. Lipo, and P. C. Krause, "Stability analysis of a symmetrical induction machine", IEEE Trans. Power App. Syst., vol. PAS-88, no. 11, pp. 1710-1717, Nov. 1969.

[8] C. P. Steinmetz, "Power control and stability of electric generating stations", AIEE Trans., vol. XIX, Part II, pp. 1215-1287, July 1920.

[9] A. Samii, A. Akram, and H. Ardiny, "Comparison of PI and Adaptive Fuzzy Controllers for Position Tracking of Servo System with Variable Loaded BLDC Motor." in 2022 10th RSI International Conference on Robotics and Mechatronics (ICRoM). IEEE, 2022.

[10] A. Samii, F. Lotfi, and H. D. Taghirad, “Optimization of Battery Life and State of the Charge in an Electric Motorcycle Braking System,” in 2021 9th RSI International Conference on Robotics and Mechatronics (ICRoM), 2021, pp. 203–209.

[11] M. Pavella and P. G. Murthy, Transient Stability of Power Systems: Theory and Practice, NY, New York, 1994.

[12] H. Yaghobi, "Transient stability enhancement of power system with instability tolerant synchronous generator", IET Generation, Transmission & Distribution, vol. 14, no. 21, pp. 4654-65, 2020.

[13] P. Kundur, J. Paserba, V. Ajjarapu, G. Andersson, A. Bose, C. Canizares, et al., "Definition and classification of power system stability", IEEE Trans. Power Syst., vol. 19, no. 3, pp. 1387-1401, 2004.

[14] R. G. Harley and B. Adkins, "Stability of synchronous machine with divided winding rotor", Proc. I.E.E., vol. 117, pp. 933-947, 1970.

[15] M. Eremia and M. Shahidehpour, Handbook of Electrical Power System Dynamics: Modeling Stability and Control, Hoboken, NJ, USA: Wiley, vol. 92, 2013.

[16] S. Ghafouri, M. A. Hajiahmadi, M. Firouzi, G. B. Gharehpetian, S. Mobayen, and P. Skruch, "Improving Transient Stability of a

Synchronous Generator Using UIPC with a Unified Control Scheme," Energies, vol. 15, no. 16, pp. 6072, 2022.
[17] H. M. Yassin, R. R. Abdel-Wahab, and H. H. Hanafy, "Active and reactive power control for dual excited synchronous generator in wind applications," IEEE Access, vol. 10, pp. 29172-29182, 2022.
[18] G. Xu, Z. Li, Z. Wang, W. Li, Y. Zhan, H. Zhao, et al., "Power tracking excitation control and its parameter optimization of dual-excited synchronous generator," IEEE Trans. Ind. Appl., vol. 58, no. 6, pp. 7099-7109, 2022.
[19] G. Xu, Y. Fu, Y. Zhan, Z. Wang, H. Zhao, and Y. Zhang, "Influence of Different Rotor Damping Structures on Dynamic Characteristic of Dual-Excited Synchronous Generator with Excitation Control," IEEE Trans. Ind. Appl., 2023.
[20] G. Xu, L. Wang, Z. Li, Z. Li, H. Zhao, Y. Zhan, et al., "Improvement of Reactive Power Consumption Ability for Dual-Excited Synchronous Condenser," IEEE Trans. Ind. Appl., 2024.
[21] G. Wang, L. Fu, Q. Hu, C. Liu, and Y. Ma, "Transient synchronization stability of grid-forming converter during grid fault considering transient switched operation mode," IEEE Trans. Sustain. Energy, 2023.
[22] P. Subramaniam and 0. P. Malik, "Dynamic stability analysis of DWR synchronous generator with feedback stabilized voltage and angle regulators", Proc. I.E.E. vol. 118, no. 12, pp. 1768-1774, 1971.
[23] B.N. Sarkar, V.K. Verma, and P. Mukhopadhyay, "Effect of field failure of a D.W.R. generator", Proc. I.E.E. vol. 127, no. 2, pp. 82-89, 1980.
[24] H. Mangel, G. Barbier, Y. Shakaryan, Y. Vinitzky, and J. M. Kauffmann, "Influence of field windings positions on two-axis excitation generators transient behavior", 1997 IEEE International Electric Machines and Drives Conference Record, pp. TC1/11.1-TC1/11.3, 1997.
[25]]C. S. Brune, R. Spe´e and A. K. Wallace, "Experimental evaluation of a variable-speed doubly-fed wind-power generation system", IEEE Trans. Ind. Applicant., vol. 30, pp. 648-655, 1994.
[26]]D. Zhou, R. Spee and G. C. Alexander, "Experimental evaluation of a rotor flux oriented control algorithm for brushless doubly-fed machines", IEEE Trans. Power Electron., vol. 12, pp. 72-78, 1997.
[27] A. Kemp et al., "Investigation of rotor current distribution in brushless doubly-fed machines", Proc. IEEE Ind. Appl. Soc. Annu. Meeting, pp. 638-643, 1996.
[28] M. S. Vicatos and J. A. Teqopoulos, "Steady-state analysis of a doubly-fed induction generator under synchronous operation", IEEE Trans. Energy Convers., vol. 4, no. 3, pp. 495-501, 1989.
[29] O. Honorati, F. Caricchi, F. Crescimbini, and G. Noia, "Stabilization and speed control of a hypersynchronous doubly-fed motor: tests and experimental results", Fifth Int. Conf. on Electrical Machines and Drivers, pp.203-207, 1991.
[30] O. Honorati, F. Caricchi, F. Crescimbini, and E. Santini, "The high speed, doubly fed synchronous motor: stabilization performances." Conference Record of the 1990 IEEE Industry Applications Society Annual Meeting. IEEE, 1990.
[31] S. E. Abo-Shady, F. I. Ahmed, A. M. El-Hakim and M. A. Badr, "Analysis of Self-Dual Excited Synchronous Machine(part(I), Development of the General Mathematical Model and Steady-state Performance Experimental Verification ", IEEE Trans. Energy Convers., vol. 3, no. 2, pp. 305-314, 1988.
[32] S. E. Abo-Shady, F. I. Ahmed and A. M. El-Hakim, "Analysis of self-dual excited synchronous machine. II. Small perturbation model and dynamic behavior." IEEE Trans. Energy Convers., vol. 3, no. 2, pp. 315-322, 1988.
[33] A. M. A. Oteafy and J. N. Chiasson, "A standstill parameter identification technique for the divided winding rotor synchronous generator", 2014 IEEE International Conference on Power and Energy (PECon), pp. 99-104, 2014.
[34] R. R. Abdel-Wahab, H. M. Yassin, and H. H. Hanafy, "Dual Excited Synchronous Generator a Suitable Alternative for Wind Applications", 2020 IEEE 14th International Conference on Compatibility, Power Electronics and Power Engineering (CPE-POWERENG), vol. 1, pp. 352-357. IEEE, 2020.
[35] S. D'Arco, L. Piegari, and P. Tricoli, "A Novel control of dual-excited synchronous machines for variable speed wind turbines", IEEE Trondheim PowerTech, 2011
[36] P. C. Krause and J. N. Towle, "Synchronous Machine Damping by Excitation Control with Direct and Quadrature Axis Field Winding", IEEE Transactions, vol. PAS-88, pp. 1266-1274, 1969.
[37] C. M. Ong, Dynamic Simulation of Electric Machinery, NJ, Englewood Cliffs: Prentice-Hall, 1998.
[38] J. C. Peqqueña, E. Ruppert and M. T. Mendoza, “On the synchronous generator parameters determination using dynamic simulations based on IEEE standards”, 2010 IEEE International Conference on Industrial Technology, pp. 386-391, 2010.